Journal of Alloys and Compounds 507 (2010) 391–398

Contents lists available at ScienceDirect

Journal of Alloys and Compounds

journal homepage: www.elsevier.com/locate/jallcom

Fe concentration dependent transport properties of LiI–AgI–B_2O_3 glass system

K. Srilatha [a], K. Sambasiva Rao [b], Y. Gandhi [a], V. Ravikumar [a], N. Veeraiah [a,*]

[a] Department of Physics, Acharya Nagarjuna University—Nuzvid Campus, College Road, Nuzvid 521 201, A.P., India
[b] Department of Physics, J.K.C. College, Guntur 522 006, A.P., India

ARTICLE INFO

Article history:
Received 29 June 2010
Received in revised form 4 August 2010
Accepted 4 August 2010
Available online 11 August 2010

Keywords:
DC conductivity
Dielectric properties
LiI–AgI–B_2O_3 glass system

ABSTRACT

LiI–AgI–B_2O_3 glasses mixed with different concentrations of Fe_2O_3 (ranging from 0 to 2.0 mol%) were prepared. DC conductivity and dielectric properties over a range of temperature and also optical absorption and ESR spectral studies have been investigated. The optical absorption and ESR studies have indicated that iron ions do exist in both Fe^{2+} and Fe^{3+} states and the reduction ratio is the highest in the samples containing 0.9 mol% of Fe_2O_3. The analysis of the results of DC conductivity has indicated that $T > \theta_D/2$, the small polaron hopping model seems to be fit and the conduction is adiabatic in nature. These results further indicated that there is a mixed conduction (both ionic and electronic) and the ionic conduction seems to prevail over polaron hopping in the glasses containing Fe_2O_3 more than 0.9 mol% of Fe_2O_3. The variations of dielectric constant and loss with temperature have been analyzed on the basis of space charge polarization. The low temperature part of AC conductivity is explained based on the quantum mechanical tunneling model.

1. Introduction

Study of electrical properties of solid electrolytes has received wide attention due to their potential applications in solid state ionic devices such as fuel cells, gas sensors, electrochemical capacitors, electrochromic displays, analog devices, cathodes in electro chemical cells, smart windows, etc. [1–4] The conductivity of LiI–AgI mixed glasses especially, has been the subject of extensive investigation in recent years as a quest for new solid electrolytes with super ionic properties [5,6]. The silver/lithium ions surrounded by iodide ions diffuse very rapidly and are the main contributors of the conductivity in the glasses; on the other hand, the silver ions interlocked with the oxide glass network are almost immobile and contribute poorly to the conductivity. Further, when these glasses are doped with multivalent transition metal ions like iron, mixed electronic and ionic, pure electronic or pure ionic conduction is expected depending upon the composition of the glass constituents. Electronic conduction in this type of materials is predicted due to polaron hopping between different valent states of transition metal ions, where as the ionic conduction is expected due to the diffusion of Li and Ag ions.

Among various transition metal ions, the iron ions are considered as effective and useful dopant ions owing to the fact that they exist in different valence states with different coordinations simultaneously in the glass network; for example as Fe^{3+} with both tetrahedral and octahedral and as Fe^{2+} with octahedral environment [7]. The content of iron in different environments and in different valence states existing in the glass however depends on the quantitative properties of modifiers and glass formers, size of the ions in the glass structure, their field strength, mobility of the modifier cation, etc. Hence, the connection between the state and the position of the iron ion and the electrical properties of the host glass containing highly mobile ions like Ag^+ and Li^+ is expected to be highly interesting. Both Fe^{3+} and Fe^{2+} ions are well-known paramagnetic ions. Fe^{2+} ion exhibits a large magnetic anisotropy due to its strong spin–orbit interaction of the 3D orbital whereas such anisotropy energy of Fe^{3+} ions is small because its orbital angular momentum is zero. Several recent works on the valence states and the influence of iron ions on the physical properties including electrical properties of a number of glasses are available in the literature [8–11]. Mogus Milancovic and her group have carried out extensive investigations that include Mossabauer spectra and DC conductivity studies recently on the glasses containing iron ions [12,13].

In spite of the fact that a considerable number of studies are available on LiI–AgI mixed glasses including lithium silver borate glasses [14], the conductivity studies as such on LiI–AgI–B_2O_3 glasses containing transition metal ions like iron are very rare and hence still there is a lot of scope to investigate the role played by iron ions on the conduction mechanism in these glasses. Further, dielectric measurements on ionic materials also give useful information about dynamical processes involving ionic motion and polaron transfer. It is known that the conductivity of glassy materials is frequency dependent, so that the diffusivity of the mobile ions

* Corresponding author. Tel.: +91 8656 235551; fax: +91 8656 235551.
E-mail address: nvr8@rediffmail.com (N. Veeraiah).

0925-8388/$ – see front matter © 2010 Elsevier B.V. All rights reserved.
doi:10.1016/j.jallcom.2010.08.016

Table 1
Various physical parameters of LiI–AgI–B_2O_3:Fe_2O_3 glasses.

Glass	F_0	F_3	F_6	F_9	F_{12}	F_{15}	F_{20}
Density (g/cm^3)	2.6749	2.6781	2.6807	2.6845	2.6875	2.6902	2.6949
Fe ion conc. N_i (10^{20} ions/cm^3)	–	0.5	1.00	1.50	2.01	2.51	3.35
Inter–ionic distance of iron ions R_i (Å)	–	27.10	21.51	18.79	17.07	15.84	14.39
Polaron radius R_p (Å)	–	10.91	8.66	7.57	6.88	6.38	5.80

is not entirely characterized by the single steady state parameter σ_{DC} quantifying DC conductivity.

The main objective of this paper is to explore the changes in conduction mechanism that take place with the varied oxidation states of iron ions in the glass network and the role of silver and lithium ions in this process by a systematic study on DC conductivity and dielectric properties (viz., dielectric constant, loss and AC conductivity over a wide range of frequency and temperature) of LiI–AgI–B_2O_3 glasses mixed with varied concentrations of Fe_2O_3 from 0 to 2.0 mol%. Auxiliary experimental data viz., optical absorption and ESR that help to have some pre-assessment over the valence states of iron ions and their environment in the glasswork have also been reported.

2. Experimental

For the present study, a particular compositions (39−x) LiI–1.0 AgI–60 B_2O_3:xFe_2O_3 with seven values of x ranging from 0 to 2.0 is chosen. The detailed compositions are as follows:

F_0: 39 LiI–1.0 AgI–60 B_2O_3
F_3: 38.7 LiI–1.0 AgI–60 B_2O_3: 0.3 Fe_2O_3
F_6: 38.4 LiI–1.0 AgI–60 B_2O_3: 0.6 Fe_2O_3
F_9: 38.1 LiI–1.0 AgI–60 B_2O_3: 0.9 Fe_2O_3
F_{12}: 37.8 LiI–1.0 AgI–60 B_2O_3: 1.2 Fe_2O_3
F_{15}: 37.5 LiI–1.0 AgI–60 B_2O_3: 1.5 Fe_2O_3
F_{20}: 37.0 LiI–1.0 AgI–60 B_2O_3: 2.0 Fe_2O_3

Analytical grade reagents of H_3BO_3, LiI, AgI and Fe_2O_3 powders in appropriate amounts (all in mol%) were thoroughly mixed in an agate mortar and melted in a platinum crucible at 900 ± 10 °C in a PID temperature controlled furnace for about 1 h. The resultant bubble free melt was then poured in a brass mould and subsequently annealed at 250 °C. The amorphous nature of the samples was verified by X-ray diffraction technique (using Xpert's PRO panalytical X-ray diffractometer with CuK_α radiation).

The density of the glasses was determined using Ohaus digital balance Model AR2140 to an accuracy of ±0.0001 by the standard principle of Archimedes' with o-xylene (99.99% pure) as the buoyant liquid. Thermal analysis of these samples was carried out by TA instruments Model Q20 V24.2 Build 107. Heating rate was 10 °C/min, in the temperature range 30–750 °C. Infrared transmission spectra were recorded on a JASCO-FT/IR-5300 spectrophotometer with a resolution of 0.1 cm^{-1} in the spectral range 400–2000 cm^{-1} using potassium bromide pellets (300 mg) containing pulverized sample (1.5 mg). These pellets were pressed in a vacuum die at ~680 MPa. The optical absorption spectra of the glasses were recorded at room temperature in the spectral wavelength range covering 400–1200 nm with a spectral resolution of 0.1 nm using JASCO Model V-670 UV-vis-NIR spectrophotometer. The electron spin resonance (ESR) spectra of the fine powders of the samples were recorded at liquid nitrogen temperature on JEOL JES-TES100 X-band EPR spectrometer. The details of the dielectrics and DC conductivity measurements are similar to those reported in our earlier papers. The dielectric constant could be measured to an accuracy of 0.001 and the loss is measured to an accuracy of 10^{-4} [15,16].

3. Results

From the measured values of density d and calculated average molecular weight $\bar{M}$, various physical parameters such as iron ion concentration N_i and mean iron ion separation r_i of these glasses are evaluated using the conventional formulae and are presented in Table 1.

Fig. 1 represents differential scanning calorimetric (DSC) scan for one of the glasses (F_3) of LiI–AgI–B_2O_3:Fe_2O_3 series; DSC trace indicate a typical glass transitions with the inflection point between 320 and 335 °C followed by a well-defined exothermic effect due to crystallization temperature (T_C) between 380 and 410 °C. The traces of all other glasses exhibited similar behaviour. The parameter $T_C - T_g$, that gives the information on the glass forming ability exhibited a decreasing trend with increase in the content of Fe_2O_3 up to 0.9 mol% and beyond this concentration it is found to increase (inset of Fig. 1).

The optical absorption spectra of LiI–AgI–B_2O_3 glasses doped with different concentrations of Fe_2O_3 recorded in the wavelength region 300–1100 nm are shown in Fig. 2. The absorption edge observed at 362 nm for the glass doped with 0.3 mol% of Fe_2O_3 is found to be shifted to slightly higher wavelength side with increase in the concentration of Fe_2O_3 up to 0.9 mol%; beyond this concentration, the edge showed signs of blue shift. The spectrum of glass F_3 exhibited three absorption bands at 776 (Oh_1), 566 (Oh_2) and 528 nm (T_d) identified due to transitions of Fe^{3+} (d^5) ions; additionally, a band at 976 nm, identified due to transition of Fe^{2+} (d^6) ions [17] is also located. With the gradual increase in the concentration of Fe_2O_3 up to 0.9 mol%, the intensity of bands due to Fe^{3+} ions has been observed to decrease with the shift of metacenters towards slightly higher energy; further with the increase of the concentration of Fe_2O_3 up to 0.9 mol%, the band due to Fe^{2+} ions is observed to grow at the expense of bands due to Fe^{3+} ions (inset of Fig. 2). From the observed absorption edges, we have evaluated the optical band gaps (E_0) of these glasses by drawing Urbach plot between $(\alpha\hbar\omega)^{1/2}$ and $\hbar\omega$. Fig. 3 represents the Urbach plots of all these glasses in which a considerable part of each curve is observed to be linear. From the extrapolation of the linear portion of these curves, the values of optical band gap (E_0) are determined and presented in Table 2. The value of optical band gap is found to be the lowest for the glass F_9 (inset of Fig. 3).

ESR spectrum for one of the LiI–AgI–B_2O_3:Fe_2O_3 glass series (F_3) recorded at room temperature is shown in Fig. 4. The spectrum exhibited an intense signal centered at about $g \sim 2.0$. The variation of intensity and the half width of this signal with the concentration of Fe_2O_3 is shown as the inset of Fig. 4. The curves exhibited a downward kink at x = 0.9 mol%. Additionally, a weak signal at about $g \sim 4.3$ could be detected in the spectra of all the glasses.

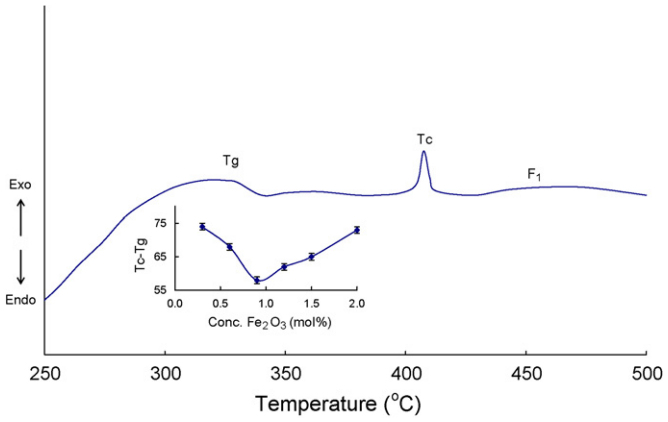

Fig. 1. DSC Trace of LiI–AgI–B_2O_3 glass doped with 0.3 mol% of Fe_2O_3 and inset shows the variation of the parameter $T_C - T_g$ with the concentration of Fe_2O_3.

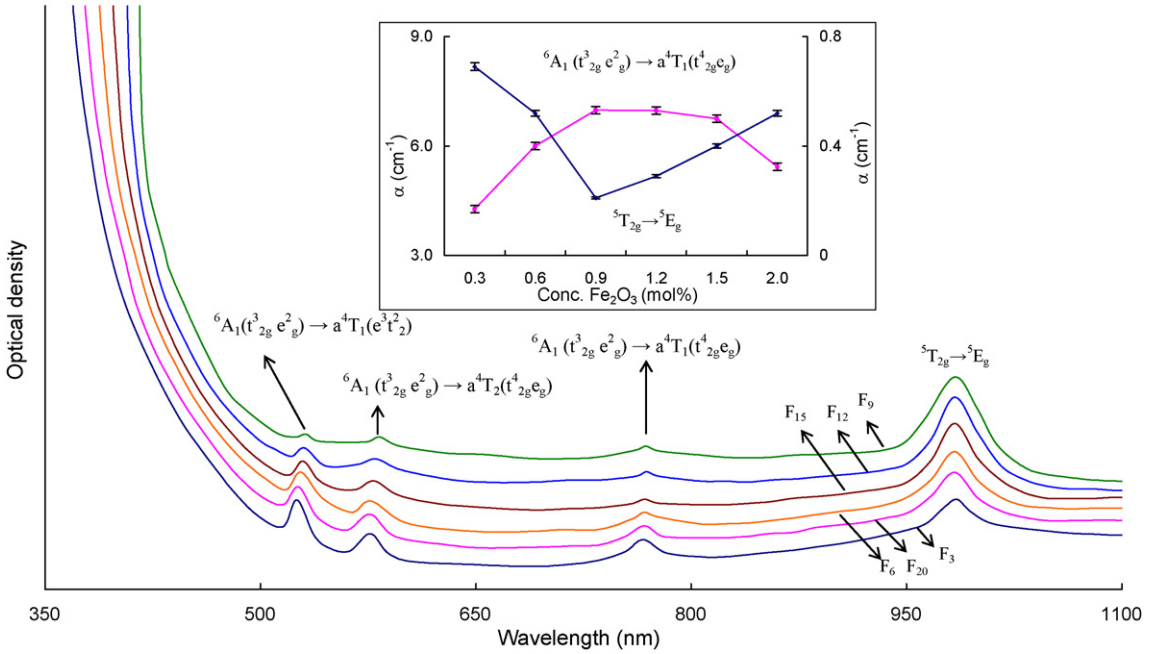

Fig. 2. Optical absorption spectra of LiI–AgI–B_2O glass doped with different concentrations of Fe_2O_3. Inset represents the variation of the peak absorption intensity of Fe^{3+} and Fe^{2+} bands.

Table 2
Summary of data on optical absorption spectra of LiI–AgI–B_2O_3:Fe_2O_3 glasses.

Glass	Cut-off wavelength (nm)	Band positions (nm)				E_0 (eV)
		$^6A_1(t^3_{2g}e^2_g) \rightarrow a^4T_1(e^3t^2 2)(O_{h1})$	$^6A_1(t^3_{2g}e^2_g) \rightarrow a^4T_2(t^4_{2g}e_g)(O_{h2})$	$^6A_1(t^3_{2g}e^2_g) \rightarrow a^4T_1(t^4_{2d}e_g)(T_d)$	$^5T_{2g} \rightarrow {}^5E_g$	
F_3	389	528	597	782	976	3.27
F_6	394	527	586	767	985	3.16
F_9	417	521	576	768	999	2.97
F_{12}	409	524	579	769	989	3.02
F_{15}	402	526	585	772	985	3.08
F_{20}	394	527	588	774	983	3.24

Fig. 5 represents the variation of ($\sigma_{DC}T$) with $1/T$ for LiI–AgI–B_2O_3 glasses doped with different concentrations of Fe_2O_3. The plots clearly indicate that the DC conductivity obeys Arrhenius relation. In the concentration range of investigation of Fe_2O_3, the measured conductivities are found to vary in the range 10^{-6} to 10^{-3} ohm^{-1} cm^{-1} in the high temperature region. The figure further indicates the deviations in linear plots (at $T = \theta_D/2$, i.e., half of the Debye temperature). The activation energy evaluated from these graphs in the high temperature region is found to decrease with increase in the concentration of Fe_2O_3 up to 0.9 mol% and there after it is found to increase (inset of Fig. 5 and Table 3). Fig. 6 presents isotherms of DC conductivity with the concentration of Fe_2O_3; the conductivity is increased at faster rates with increase in the concentration of iron ions up to 0.9 mol% and then it is decreased for further increase of iron ion content.

The dielectric constant ε' and loss tan δ at room temperature (≈30 °C) of pure LiI–AgI–B_2O_3 glasses at 100 kHz are measured to be 12.4 and 0.005, respectively. The temperature dependence of ε' of the glasses containing different concentrations of Fe_2O_3 at 1 kHz is shown in Fig. 7 and at different frequencies of glass F_9 is shown as the inset of the same figure. The value of ε' is found to exhibit a considerable increase at higher temperatures especially at lower frequencies; the rate of increase of ε' with temperature is found to be the highest for the glass doped with 0.9 mol% of Fe_2O_3.

The temperature dependence of tan δ of all the glasses measured at a frequency of 10 kHz is presented in Fig. 8. In the inset of the same figure, the variation of tan δ for one of the glasses (glass containing 0.9 mol% of Fe_2O_3), at different frequencies is presented. These curves have exhibited distinct maxima; with increasing frequency the temperature maximum shifts towards higher temperature and with increasing temperature the frequency maximum shifts towards higher frequency, indicating the dielectric relaxation character of dielectric losses of these glasses. The relaxation intensity is found to be the maximum for the glass mixed with 0.9 mol%

Table 3
Summary of data on conductivity studies of LiI–AgI–B_2O_3:Fe_2O_3 glasses.

Glass	W_{DC} (eV)	W_H (eV)	J_0 (eV)	J (eV)	W_{AC} (eV)	$N(E_F)$ ($\times 10^{20}$ eV^{-1}/cm^3)	AE for dipoles (eV)
F_3	0.612	0.365	0.091	0.0004	0.489	1.39	2.77
F_6	0.466	0.274	0.069	0.00101	0.392	1.74	2.31
F_9	0.301	0.180	0.045	0.0019	0.261	3.12	2.28
F_{12}	0.376	0.219	0.055	0.0027	0.326	2.52	2.57
F_{15}	0.43	0.257	0.064	0.0027	0.301	2.06	2.74
F_{20}	0.522	0.312	0.078	0.0044	0.435	1.51	2.82

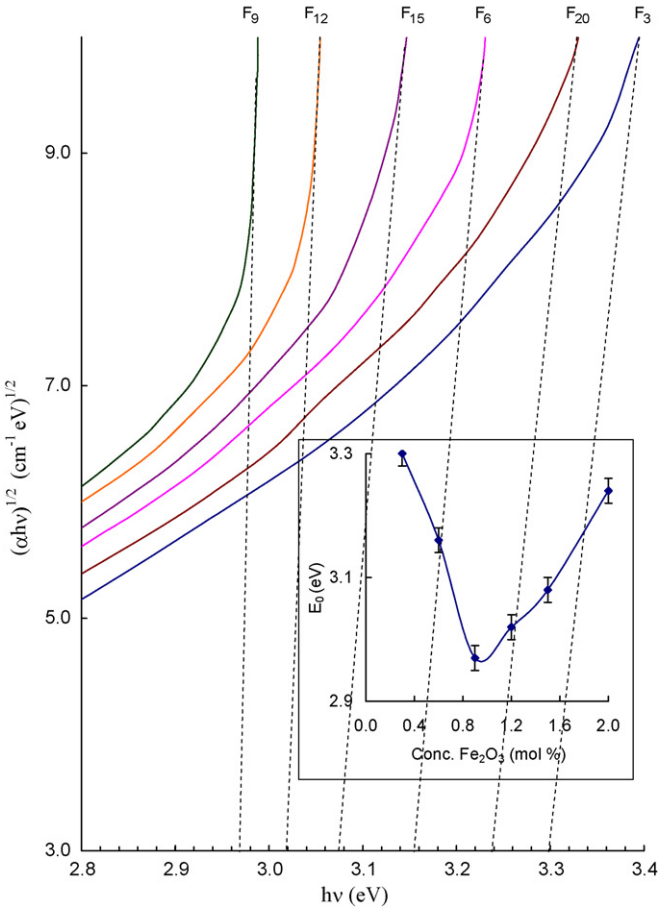

Fig. 3. Urbach plots for the evaluation of optical band gap. Inset represents the variation of the optical band gap with the concentration of Fe_2O_3.

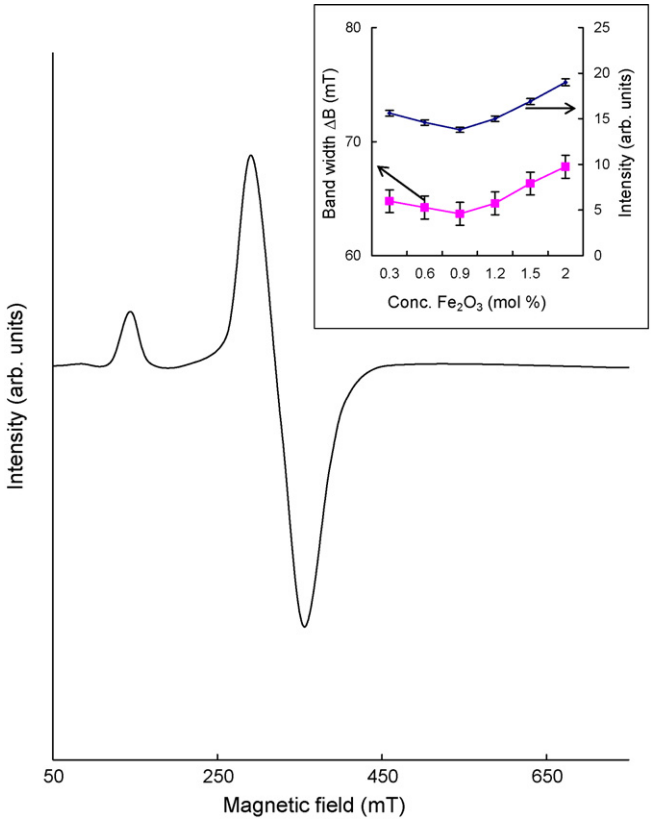

Fig. 4. ESR signal for the glass F_3 recorded at room temperature. Inset represents variation of intensity and half width of the signal with the concentration of Fe_2O_3.

and minimal for the glasses F_{12} to F_{15}. From these curves, the effective activation energy, W_d, for the dipoles is calculated for different concentrations of Fe_2O_3 and presented in Table 3; the activation energy is found to be the lowest for the glass F_9 and the highest for the glass F_3.

The AC conductivity σ_{AC} is evaluated at different temperatures from the values of dielectric constant and loss using the conventional equation and its variation with $1/T$ for all the glasses at 100 kHz is presented in Fig. 9. Similar to that of DC conductivity, σ_{AC} is also found to be the highest for the glasses containing 0.9 mol% of Fe_2O_3 at any temperature. The variation of AC conductivity with temperature exhibited a plateau up to 110 °C and there after (beyond the relaxation region) it is increased rapidly exhibiting the highest rate of increase for the glass F_9. From these plots, the activation energy for the conduction in the high temperature region over which a near linear dependence of $\log \sigma_{AC}$ with $1/T$ could be observed is evaluated and presented in the Table 3.

4. Discussion

B_2O_3 is a well-known network former, participates in the network forming with BO_3 and BO_4 structural units. AgI and LiI do act as modifiers like any conventional modifiers and create bonding defects. In some of the recent investigations it has also been reported that Ag^+ and Li^+ ions in oxysalt glass matrices experience mixed oxygen–iodine coordination and do not induce any defects in the glass network [18–20]. According to this model AgI and LiI mainly act to expand the glass network, which leads to the increase in the accessible volume for the fraction of mobile Ag^+ and Li^+ ions

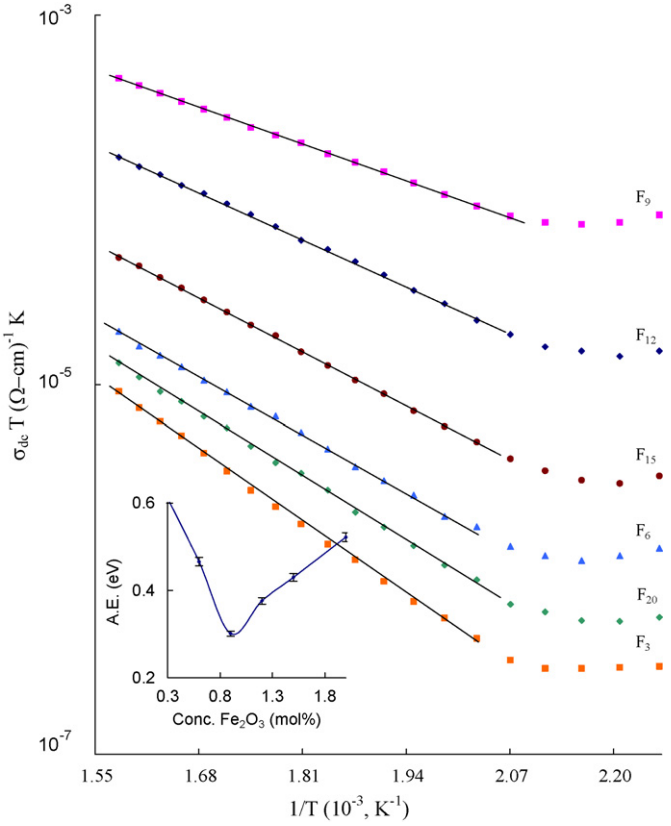

Fig. 5. Variation of ($\sigma_{DC}T$) with $1/T$ for LiI–AgI–B_2O_3:Fe_2O_3 glasses. Inset represents the variation of activation energy with the concentration of Fe_2O_3.

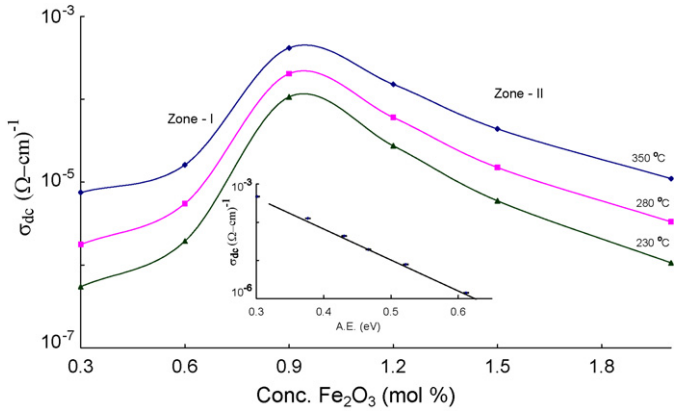

Fig. 6. DC conductivity isotherms of LiI–AgI–B_2O_3:Fe_2O_3 glasses. Inset shows the variation of conductivity (at 623 K) with the activation energy.

that act as modifiers. In fact a general relation between the network expansion and the conductivity enhancement for a large variety of alkali–halide mixed oxide glasses has been reported [21].

Iron ions are expected to exist mainly in Fe^{3+} state in LiI–AgI–B_2O_3 glass network. However, regardless of the original oxidation state of the iron in the starting glass batch, the final glass contains both Fe^{3+} and Fe^{2+} ions [22]. The speciation of iron in these glasses is controlled by the following reversible reaction:

$$4Fe_{melt}{}^{3+} + 2O_{melt}{}^{2-} \rightleftharpoons 4Fe_{melt}{}^{2+} + O_{2\,melt\,atm}.$$

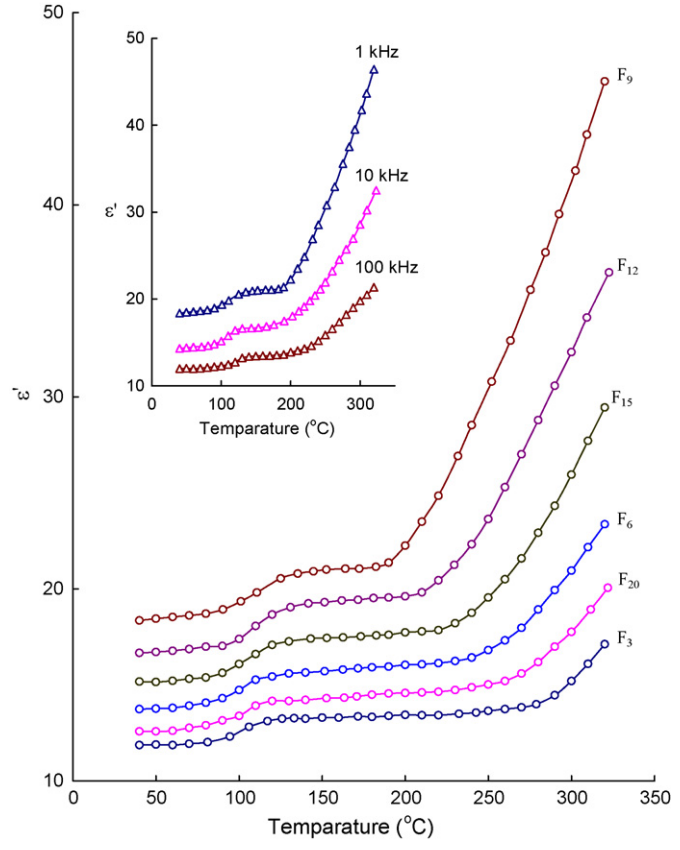

Fig. 7. A comparison plot of variation of dielectric constant with temperature at 1 kHz for LiI–AgI–B_2O_3 glass doped with various concentrations of Fe_2O_3. Inset shows the variation of dielectric constant with temperature at different frequencies for the glass F_9.

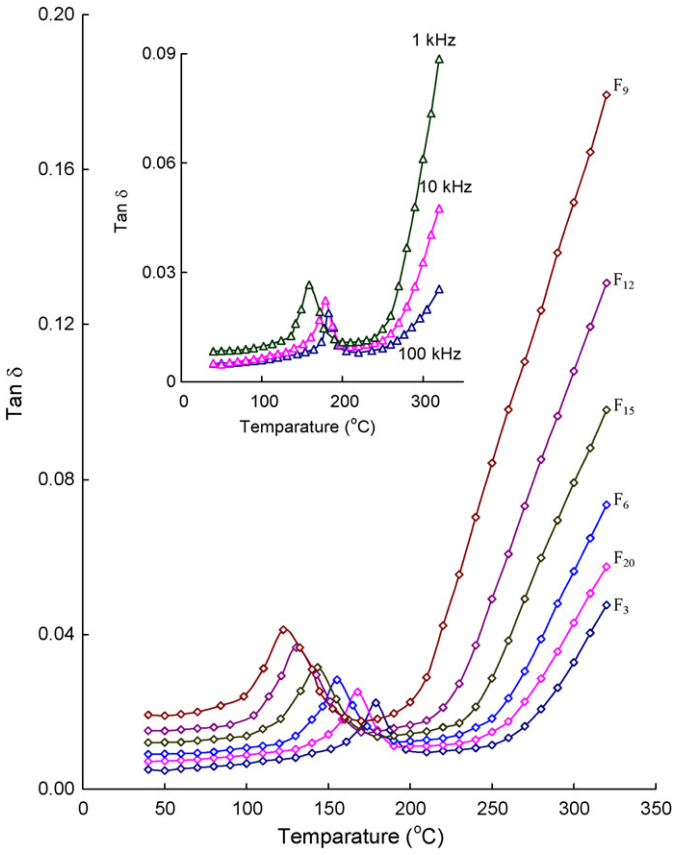

Fig. 8. A comparison plot of variation of dielectric loss with temperature at 10 kHz for LiI–AgI–B_2O_3 glasses doped with various concentrations of Fe_2O_3. Inset shows the variation of dielectric loss with temperature at different frequencies for the glass F_9.

Fe^{3+} ions are expected to occupy both tetrahedral and octahedral positions in the glass network. Nevertheless, the fourfold coordination of Fe^{3+} is observed to be more common than the sixfold coordination in many of the glasses [23]. Both of these Fe^{3+} sites can be considered as substitutional and subjected to strong interaction

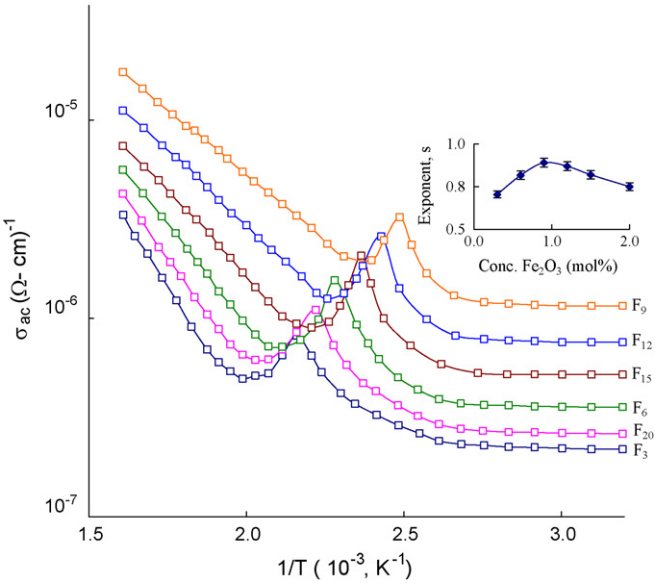

Fig. 9. Variation of σ_{AC} with $1/T$ for LiI–AgI–B_2O_3:Fe_2O_3 glasses at 100 kHz. Inset represents the variation of frequency exponent, s with the concentration of Fe_2O_3.

between its external orbitals and the p-orbitals of the neighbouring oxygens [24] and form the linkages of the type B–O–Fe with the borate groups. Fe^{2+} ions acts as modifiers similar to Li and Ag ions.

The entry of Ag^+ into the glass network may be represented as follows:

$$B\text{–}O\text{–}Fe + AgI \rightarrow B\text{–}O^-Ag^+ + Fe\text{–}O^-Ag^+$$

As a consequence, there is a disruption in the BO_4 and FeO_4 structural units with the creation of number of non-bridging oxygens.

Recollecting the data on DSC studies, we have observed that the values of the glass transition temperature T_g and glass forming ability parameter ($T_C - T_g$) have exhibited minimal effects at 0.9 mol% of Fe_2O_3. Normally, the bond length, cross-link density and closeness of packing, are responsible for variation of these parameters. The dip observed at $x = 0.9$ (inset Fig. 1) obviously suggests a high degree of disorder in the network of glass F_9, owing to the presence of larger concentrations of Fe^{2+} ions.

Using Tanabe–Sugano diagrams for d^5 ion, the optical absorption spectra have been analyzed and the Oh_1 and Oh_2 bands are assigned to $^6A_1(t_{2g}^3e_g^2) \rightarrow a^4T_1(t_{2g}^4e_g)(O_{h1})$, $^6A_1(t_{2g}^3e_g^2) \rightarrow a^4T_2(t_{2g}^4e_g)(O_{h2})$ transitions (due to the substitutionally positioned octahedral Fe^{3+} ions) respectively where as the T_d band (tetrahedral band) is identified due to $^6A_1(e^2t_2^3) \rightarrow a^4T_1(e^3t_2^2)$ (spin forbidden) transitions of Fe^{3+} ions [25] with LF parameters, D_q (crystal field splitting energy) $\sim$1270 cm^{-1} and Racah inter electronic repulsion parameters $B \sim 840\ cm^{-1}$. The band observed at 970 nm is identified due to $^5T_{2g} \rightarrow {}^5E_g$ transition of Fe^{2+} (d^6) ions [26].

When the concentration of Fe_2O_3 is increased up to 0.9 mol%, the band due to $^5T_{2g} \rightarrow {}^5E_g$ transition prevails over the other transitions from $^6A_1$ ground state and for further increase of Fe_2O_3 a reversal trend is observed; such variations indicates that, trivalent iron ions, that participate in the glass network forming, dominate over the divalent ions in the glasses F_{12} and F_{15} where as in the glass F_3 to F_9 the concentration of Fe^{2+} ions is higher. Further, these Fe^{2+} ions are expected to occupy only interstitial positions since the ratio of cation–oxygen radii is 0.63 for Fe^{2+} ion, which is far from the value of 0.19 to be possessed by an ion to occupy tetrahedral or substitutional sites [24] and create more disorder by creating dangling bonds in the glass network. The optical activation energy associated with the octahedral band of Fe^{3+} ions viz., $^2B_{2g} \rightarrow {}^2B_{1g}$ is increased from 2.33 eV (sample F_3) to 2.38 eV (sample F_9) where as the energy of Fe^{2+} ion transition band is decreased from 1.27 eV (sample F_3) to 1.241 (sample F_9); this is clearly a characteristic signal of inter valence transfer or a polaronic type of absorption. To be more specific, the associated electrons are trapped at shallow sites within the main band gap and yet have smaller wave-function radii. In terms of polaronic perception, this kind of situation is only possible if the local potential fluctuation is small as compared to the transfer integral, j. A small overlap between electronic wave functions (corresponding to adjacent sites) due to strong disorder is contributive to polaron formation. So from the polaronic viewpoint, the electron delivered by the impurity atom at the Fe^{3+} site converts this into a lower valence state Fe^{2+}, and at the next stage, the trapped electron at this Fe^{2+} site is transferred to the neighboring new Fe^{3++} site by absorbing a photon energy. Thus the optical absorption in the glass samples is dominated by polaronic transfer between the Fe^{2+} and Fe^{3+} species [27,28].

With the increase in the concentration of Fe^{2+} ions and the entry of Ag^+ and Li^+ ion in the glass network, a large number of donor centers are created, and subsequently, the excited states of localized electrons originally trapped on Fe^{2+} sites begin to overlap with the empty 3d states on the neighboring Fe^{3+} sites, and as a result, the impurity or polaron band becomes more extended into the main band gap. This new polaronic development might have shifted the absorption edge to the lower energy which leads up to a significant shrinkage in the band gap as the concentration of Fe_2O_3 is increased up to 0.9 mol%.

The ESR spectra of these glasses have exhibited two signals cantered at $g = 4.2$ and 2.0. These two resonance lines have been discussed at length by many investigators [29,30]. The absorption at $g = 4.2$ is identified to the isolated Fe^{3+} ions in the orthorhombic crystal field, arises from tetrahedral environment and the line at $g = 2.0$ is predicted due on the Fe^{3+}–O–Fe^{3+} spin pair [31]. The variations in the ESR line-shape and the intensity can be explained on the basis of variations in the concentration of Fe^{3+} ions. In the present case, the change in the Fe^{3+}/Fe_{tot} ratio seems to be one of the reasons for the variations in the line-shape. Additionally other factors, e.g., the jumping frequency of the charge carriers ($Fe^{2+} \rightarrow Fe^{3+}$) which is proportional to $\exp(-W/kT)$, where $W = 1/2\ W_D + W_H$ (W_D is the mean energy difference between adjacent iron sites due to the disordered nature of the glass and W_H is the activation energy for the hopping process of the polarons between two identical sites), also accounts for such variations. In the case of samples containing $Fe_2O_3 > 0.9$ mol%, it is possible to suppose that the leading term is W_H, and that the jumping rate of the polaron is high; this fact, together with the relative high concentration of the Fe^{3+} species accounts for the intense ESR signal for the samples F_{12} to F_{20}.

Thus the measurements on optical absorption and ESR spectra clearly suggest the increasing proportions of trivalent iron ions as the concentration of Fe_2O_3 is increased beyond 0.9 mol% in the glass network or in other words the redox ratio (conc. Fe^{2+} ions/conc. Fe^{3+} ions) is the highest for the glass F_9 and decreases gradually form the glass F_9 to F_{20}.

When a plot is made between $\log \sigma_{DC}$ vs activation energy for conduction, a near linear relationship is observed (inset of Fig. 6); this observation suggests that the conductivity enhancement is also related to the thermally stimulated mobility of the charge carriers in the high temperature region. The maximal effect observed at $x = 0.9$ mol% in the isotherms of DC conductivity suggests that there is a changeover of conduction mechanism at this point.

The DC conductivity of the LiI–AgI–B_2O_3:Fe_2O_3 glasses for the hopping of the small polarons is given by [32,33]:

$$\sigma_{DC} = \frac{\nu_o N_i e^2 R^2 C}{kT}(1 - C)\exp(-2\alpha R)\exp\frac{-W}{kT} \quad (1)$$

where N_i is the concentration of Ag^+ ions, ν_0 is the phonon frequency ($=\theta_D$ K/h); C is the mole fraction of the sites occupied by electron and α is the electron wave function decay constant R is the mean separation between iron ions. The term $\exp(-\alpha R_i)$ represents electron overlap integral. The variation of $\sigma_{DC}T$ with $1/T$ shown in Fig. 5 is well in accordance with Eq. (1).

Additionally, as has been mentioned earlier, the conductivity enhancement with temperature for a given composition of the glass suggests the contribution of ionic transport to the conduction in addition to the polaron hopping. The decrease in activation energy and increase in conductivity with iron ion content up to 0.9 mol% (Figs. 5 and 6) may be due to higher rate of polaron hopping ($Fe^{2+} \leftrightarrow Fe^{3+}$) and ionic transport. Though electronic and ionic conductivities are not separated but the observed trend of increase of conductivity and decrease of activation energy (for the glass containing Fe_2O_3 below 0.9 mol%) (zone-I) and decrease of conductivity and increase of activation energy (for the glass containing Fe_2O_3 beyond 0.9 mol%) (zone-II) indicates different conduction mechanisms on the two sides of this composition. This type of composition dependence of isothermal conductivity is quite conventional in the glasses containing mobile monovalent cations (like Li^+ and Ag^+) and transition metal ions like iron.

Based on earlier NMR studies [18,34,20] on the oxide glasses containing AgI, one can imagine that a part of Ag^+ and Li^+ ions have oxygen and iodine in their coordination sphere, which do not affect

the borate glass network. These studies have also revealed that the fraction of the Ag^+ and Li^+ ions contributing to the transport process is independent of temperature and the content of AgI and LiI in the glass matrix. Nevertheless, Fe^{2+} ions act as modifiers, create dangling bonds and increase the accessible free volume with the enhancement of the number of conduction pathways available for the migration of Ag^+ and Li^+ ions; in other words, the presence of higher proportions of Fe^{2+} ions in the glass network lead to decrease the electrostatic binding energy that traps Ag^+ and Li^+ ions to the charge compensating oxygen ions and also decrease in the strain energy for the easy passage of these ions; such decrease lead to a substantial decrement in the jump distance of Ag^+ and Li^+ ions. This is principal factor for the increase in the conductivity in the zone-I in addition to polaron hopping. To be more quantitative, the ionic conduction in this type of glasses is the height of the energy barrier that the conducting ions (Li^+ and Ag^+ in this case) should overcome. According to Anderson and Stuart model [35], the two principal controlling factors are, the electrostatic binding energy that arises from Columbic force acting on the ions as they move away from their charge compensation sites and the migration energy against the mechanical forces acting on the ion as it dilates the structure sufficiently to allow it to move between equilibrium sites in the glass network.

Further, the polarons involved in the process of transfer from Fe^{2+} to Fe^{3+}, are attracted by the oppositely charged Ag^+ and Li^+ ions. This cation-polaron pair moves together as a neutral entity. As expected, the migration of this pair is not associated with any net displacement of the charge and thus does not contribute to electrical conductivity. As a result, there is a decrease in the conductivity, in the zone-II [36]. In other words, with the entry of network modifying Ag^+ and Li^+ ions into the glass network, the electronic paths are progressively blocked causing an inhibition of the electronic current in this region.

The activation energy W for the DC conductivity can be expressed as [37],

$$\begin{aligned} W &= W_H + \frac{1}{2}W_D \quad \text{for} \quad \frac{T > \theta_D}{2} \\ &= W_D \quad\quad\quad\quad \text{for} \quad \frac{T < \theta_D}{4} \end{aligned} \tag{2}$$

where W_H is the polaron hopping energy, W_D is the disorder energy and θ_D is the Debye temperature. The polaron hopping energy is evaluated using the equation

$$W_H = \frac{W_P}{2} = \frac{e^2}{4\varepsilon_p}\left(\frac{1}{r_p} - \frac{1}{R}\right) \tag{3}$$

and presented in Table 3. In Eq. (3) W_p is the polaron binding energy ε_p is effective dielectric constant.

To explore the nature of the hopping conduction in $LiI–AgI–B_2O_3:Fe_2O_3$ glasses a graph between $\log\sigma_{DC}$ (measured at 623 K) and the activation energy 'W_{DC}' is plotted in the inset of Fig. 6; the graph obtained is a straight line; this observation indicates that the Eq. (1) is valid. From the slope of this curve, the value of $1/kT$ is obtained and the temperature T is estimated. The value of T is found to be 615 K which is very close to the actual temperature. This observation suggests that the hopping is adiabatic and the conduction is mainly controlled by the activation energy only as represented by Eq. (2). In small polaron hopping model (SPH Model), the polaron band width J for adiabatic case is given by

$$J > \left(\frac{2kTW_H}{\pi}\right)^{1/4}\left(\frac{h\nu_0}{\pi}\right)^{1/2} \tag{4}$$

The polaron bandwidths are also calculated from the relation $J = J_0\exp(-\alpha R)$, where $J_0 = W_{H(\min)}/4$ [38] and are furnished in Table 3. From this table, it may be noted that J for all the glasses satisfies the Eq. (4) and hence the conduction may be taken as adiabatic which means there is non-compatibility between the hopping rate of polaron and phonon frequency. According to a more general polaron hopping model (where $W_D > 0$) it is the optical multi phonon that determines DC conductivity at high temperatures, while at low temperatures, charge carrier transport is via an acoustical phonon-assisted hopping process [39].

Recollecting the data on dielectric properties of $LiI–AgI–B_2O_3:Fe_2O_3$ glasses, with the gradual increase of Fe_2O_3 up to 0.9 mol% in the glass network, the values of ε', $\tan\delta$ and σ_{AC} are found to increase at any frequency and temperature and the activation energy for AC conduction are observed to decrease; this observation indicates an increase in the space charge polarization owing to the enhanced degree of disorder in the glass network [40,41] due to the presence larger proportions of Fe^{2+} ions that act as modifier.

The dielectric relaxation effects exhibited by these samples can safely be attributed to association of divalent iron with a pair of I^- or O^- ions, in analogy with the mechanism-association of divalent positive ion with a pair of cationic vacancies – in conventional glasses, glass ceramics and crystals [42,43]. The increase in the breadth and the intensity of the relaxation peaks and (for the samples F_3 to F_9) supports the view point that there is a higher concentration of divalent iron ions and also Li^+ and Ag^+ ions in these glasses that acts as modifiers. The lower values of activation energy for these samples suggest an increasing degree of freedom for dipoles to orient in the field direction.

The frequency response of real part of AC conductivity is normally described by power law dependence with s as exponent:

$$\sigma'(\omega) = \sigma_{DC}\left[1 + \left(\frac{\omega}{\omega_c}\right)^s\right], \quad 0 \le s < 1 \tag{5}$$

ω_C is the characteristic macroscopic relaxation frequency.

Within the framework of the linear-response theory, the frequency-dependent conductivity can be related to

$$\sigma(\omega) = -\frac{q^2 n_c \omega^2}{6kTH_R}\int_0^\infty \langle r^2(t)\rangle e^{-i\omega t}\mathrm{d}t \tag{6}$$

where q is the charge, n_c is the mobile ion density, $\langle r^2(t)\rangle$ is the mean square displacement of the mobile ions and H_R is the Haven ratio (lies in between 0.2 and 1.0) [44] which represents the degree of correlation between successive hops.

At short times, when the mean square displacement $\langle r^2(t)\rangle$ of ions is small then it is $\sim t^{1-s}$, the ion transport is characterized by the non-random forward–backward hopping process, under these conditions Eq. (5) modifies to

$$\sigma(\omega) \propto \omega^s \tag{7}$$

The variation of the exponent (obtained by plotting $\log\sigma(\omega)$ vs ω) is found to be the highest for the glass F_9 (inset of Fig. 9). Such increase suggests that dimensionality of conduction space is the highest for this glass [45,46].

The AC conductivity in the low temperature region (near plateau region) can be understood based on quantum mechanical tunneling model. Based on Austin and Mott's model (quantum mechanical tunneling model) [37], the density of defect energy states near the Fermi level, $N(E_F)$, at nearly temperature independent region of the conductivity (low temperature) is evaluated using

$$\sigma(\omega) = \frac{\pi}{3}e^2 KT[N(E_F)]^2\alpha^{-5}\omega\left[\ln\frac{\nu_o}{\omega}\right]^4 \tag{8}$$

where α is the electronic wavefunction decay constant, ν_0 is the phonon frequency, and presented in the Table 3. The value of $N(E_F)$, i.e., the density of defect energy, is found to increase gradually from

the sample F_3 to F_9, indicating a growing degree of disorder with increase in the content of Fe_2O_3 up to 0.9 mol% in the glass network.

5. Conclusions

LiI–AgI–B_2O_3 glasses mixed with different concentrations of Fe_2O_3 (ranging from 0 to 2.0 mol%) were prepared. DSC, optical absorption, ESR, DC conductivity and dielectric properties have been investigated. Optical absorption and ESR studies have indicated that iron ions exist in Fe^{2+} state in addition to Fe^{3+} state. DC conductivity is increased up to 0.9 mol% of Fe_2O_3 and beyond that the conductivity is found to decrease. The analysis of the DC conductivity results indicated that there is a mixed conduction (both ionic and electronic) and the ionic conduction seems to prevail over polaron hopping in the glasses containing Fe_2O_3 more than 0.9 mol%. The temperature independent part of AC conductivity is explained on the basis of quantum mechanical tunneling model.

Acknowledgement

One of the authors K. Srilatha wishes to thank UGC, Govt. of India and the Management of St. Theresa's College, Eluru for sanctioning study leave to carry out this work.

References

[1] J.W. Fergus, J. Power Sources 162 (2006) 30.
[2] H. Yoshioka, S. Tanase, Solid State Ionics 176 (2005) 2395.
[3] T. Ngai, S. Tamura, N. Imanaka, Sen. Actuators B: Chem. 147 (2010) 735.
[4] A. Karuppasamy Subrahmanyam, Thin Solid Films 516 (2007) 175.
[5] E. Kartini, T. Sakuma, K. Basar, M. Ihsan, Solid State Ionics 179 (2008) 706.
[6] A. Stéphanie, F. Nathalie, G.Y. Pascal, P. Annie, R. Michel, Mater. Sci. Eng.: B 150 (2008) 199;
A. Stéphanie, F. Nathalie, G.Y. Pascal, P. Annie, R. Michel, Micropo. Mesopo. Mater. 99 (2007) 56.
[7] M. Ghazzali, V. Langer, L. Öhrström, J. Solid State Chem. 181 (2008) 2191.
[8] N. Krishna Mohan, K. Sambasiva Rao, Y. Gandhi, N. Veeraiah, Phys. B 389 (2007) 213.
[9] A. Rajendra Kumar Singh, A. Srinivasan, Appl. Surf. Sci. 256 (2010) 1725.
[10] V. Simon, D. Eniu, M. Neumann, S. Simon, Int. J. Mod. Phys. B 18 (2004)2215.
[11] V. Simon, D. Muresan, S. Simon, Eur. Phys. J. Appl. Phys. 37 (2007) 219.
[12] A. Moguš-Milanković, V. Ličina, S.T. Reis, D.E. Day, J. Non-Cryst. Solids 353 (2007) 2659.
[13] A. Šantić, A. Moguš-Milanković, K. Furić, V. Bermanec, C.W. Kim, D.E. Day, J. Non-Cryst. Solids 353 (2007) 1070.
[14] M. Foltyn, M. Wasiucionek, J. Garbarczyk, J.L. Nowiński, Solid State Ionics 176 (2005) 2137.
[15] M. Nagarjuna, T. Satyanarayana, V. Ravi Kumar, N. Veeraiah, Phys. B 404 (2009) 3748.
[16] T. Satyanarayana, I.V. Kityk, M. Piasecki, P. Bragiel, M.G. Brik, Y. Gandhi, N. Veeraiah, J. Phys. Condens. Matter 21 (2009) 245104.
[17] S.P. Singh, R.P.S. Chakradhar, J.L. Rao, B. Karmakar, J. Alloy. Compd. 493 (2010) 256.
[18] K.K. Olsen, J. Zwanziger, Solid State Nucl. Magn. Reson. 5 (1995) 123.
[19] K.K. Olsen, J. Zwanziger, P. Hertmann, C. Jager, J. Non-Cryst. Solids. 222 (1997) 199.
[20] E.I. Kamitsos, J.A. Kaputsis, G.D. Chryssikos, J.M. Hutchinson, A.J. Pappin, M.D. Ingram, J.A. Duffy, Phys. Chem. Glasses 36 (1995) 141.
[21] J.D. Wicks, L. Borjesson, G. Bushnell-Wye, W.S. Howells, R.L. McGreevy, Phys. Rev. Lett. 74 (1995) 726.
[22] G.K. Marasinghe, M. Karabulut, C.S. Ray, D.E. Day, C.H. Booth, P.G. Allen, D.K. Shuh, Ceram. Trans. 87 (1998) 261.
[23] G.K. Marasinghe, M. Karabulut, C.S. Ray, D.E. Day, C.H. Booth, P.G. Allen, D.K. Shuh, J. Non-Cryst. Solids 249 (1999) 261.
[24] S.M.D. Nery, W.M. Pontuschka, S. Isotani, C.G. Rouse, Phys. Rev. 49 (1994) 3760.
[25] E. Baiocchi, A. Montenero, M. Bettinelli, J. Non-Cryst. Solids 46 (1981) 203.
[26] F. Albert Cotton, G. Wilkinson, C.A. Murlio, M. Bochmann, Advanced Inorganic Chemistry, John Wiley & Sons, New York, 1999.
[27] O. Cozar, D.A. Magdas, I. Ardelean, J. Non-Cryst. Solids 354 (2008) 1032.
[28] B.V.R. Chowdari, K. Radha Krishnan, J. Non-Cryst. Solids 224 (1998) 151.
[29] I. Ardelean, M. Toderas, S. Filip, J. Magn. Magn. Mater. 272 (2004) 339.
[30] D. Rusu, M.F. Carrasco, M. Toderas, I. Ardelean, J. Mod. Phys. B 19 (2005) 1821.
[31] K. Tanaka, K. Kamiya, T. Yoko, J. Non-Cryst. Solids 109 (1989) 289.
[32] N.F. Mott, J. Non-Cryst. Solids 1 (1968) 1.
[33] N.F. Mott, Phil. Mag. 19 (1969) 835.
[34] K.K. Olsen, J. Zwanziger, P. Hertmann, C. Jager, J. Non-Cryst. Solids 222 (1997) 199.
[35] O.L. Anderson, D.A. Stuart, J. Am. Ceram. Soc. 37 (1954) 573.
[36] J.C. Bazan, J.A. Duffy, M.D. Ingram, M.R. Mallace, Solid State Ionics 86 (1996) 497.
[37] I.G. Austin, N.F. Mott, Adv. Phys. 18 (1969) 41.
[38] K. Sega, Y. Kuroda, H. Sakata, J. Mater. Sci. 33 (1998) 138.
[39] J. Schnakenberg, Phys. Stat. Solidi 28 (1968) 623.
[40] A. Padmanabham, T. Satyanarayana, Y. Gandhi, N. Veeraiah, J. Alloys Compd. 88 (2009) 400.
[41] G. Murali Krishna, B. Anila Kumari, M. Srinivasa Reddy, N. Veeraiah, J. Solid State Chem. 180 (2007) 2747.
[42] P. Subbalakshmi, N. Veeraiah, Phys. Chem. Glasses 12 (2001) 307.
[43] N. Veeraiah, J. Mater. Sci. 22 (1987) 2017.
[44] H. Kahnt, J. Non-Cryst. Solids 203 (1996) 225.
[45] D.L. Sidebottom, Phys. Rev. Lett. 83 (1999) 983.
[46] S. Bhattacharya, A. Ghosh, Phys. Rev. B 70 (2004) 172203.